River Flow 2010 - Dittrich, Koll, Aberle & Geisenhainer (eds) - © 2010 Bundesanstalt für Wasserbau ISBN 978-3-939230-00-7

Flume LES of a glued spheres layer – Detailed analysis of initial motions of a single grain

M. Grünzner & P. Rutschmann
Lehrstuhl für Wasserbau und Wasserwirtschaft, Technische Universität München, Germany

ABSTRACT: Highly resolved 3D Navier-Stokes simulations using a Large Eddy turbulence approach are becoming very popular these days due to fast and yet affordable processor architectures. The following paper deals with 3D Large Eddy Simulation (LES) of a 30 cm wide flume having a bottom with glued spheres of identical diameter (1 cm). In the centre of the test reach one single and mobile sphere, representing a sediment grain, was exposed to the flow and additionally could be moved into the flow by a stamp. Different flow fields were computed as initial conditions, from which the grain was protruded into the flow. This setup corresponds to a laboratory test setup used and described by Fenton and Abbot (1977). Like in the experiment the single grain is also in the numerical test fully coupled with the fluid and therefore a complete fluid-grain-interaction (two way coupling) is enhanced. For the computations a highly resolved mesh with 1x1x1 millimeter cells was used. The paper focuses on the basics of modeling and interpreting LES as well as on the analysis of the computed flow. Furthermore the initial motion of the numerical grain is investigated in detail by observing the fluid flow forces. First results for initial motions and the application of a probabilistic approach for beginning sediment transport are discussed.

Keywords: LES, Spheres layer, Initial grain motion

1 INTRODUCTION

To improve the understanding of the physical process of sediment transport a numerical model, similar to the physical model of Fenton and Abbott (1977), were simulated. Fenton and Abbot investigated initial motion of non-cohesive bed-grain-material on an ideal packed bed. They slowly pushed a grain vertically into the flow, measured the protrusion and evaluated the relation of dimensionless exposure versus dimensionless flow induced shear. Based on Shields (1936) experiments they were able to determine the critical dimensionless shear stress of initial motion for different exposures and flow conditions. Figure 1 shows a longitudinal section of the setup used by Fenton and Abbott.

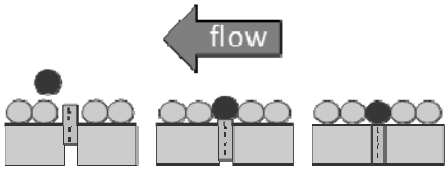

Figure 1. Schematic setup

One of the most important results of Fenton and Abbott is shown in figure 2. It shows the correlation between shields value and grain exposition for initial motion.

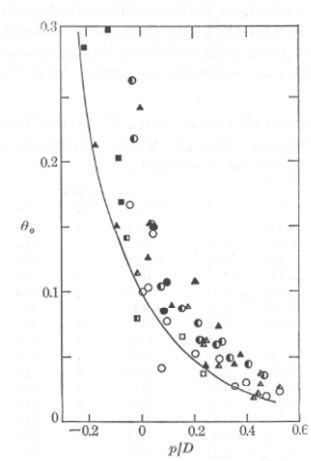

Figure 2. Correlation between grain exposition and the dimensionless threshold shear stress (taken from Fenton & Abbott 1977).

The relation p/D means the exposition which is also defined in figure 10.

The line in figure 2 is not a trend line. Fenton and Abbott interpreted their results as a kind of envelope of minimum values.

Actual, similar research is done by Braun et al. (2009)

2 NUMERICAL MODEL

For the numerical simulations the commercial three dimensional code Flow3D from Flow Science Inc., Santa Fe, were used. Flow3D uses a structured, regular and orthogonal grid to solve for the full Navier-Stokes. In order to account for turbulence effects, various turbulent models and also a Large Eddy Simulation (LES) approach are available. For the present investigation the hydrodynamics was computed using the LES option where most of the turbulent energy is resolved by the fine computational grid and for the unresolved turbulence a Smagorinsky model is used.

The General Moving Object (GMO) module of Flow3D is capable to resolve the 6 degrees of freedom (6DOF) of physical bodies. At first, the hydraulic flow field is calculated taking into account the GMOs and the resulting loads on the bodies are transferred. Then the 6DOF solver calculates the movement of the bodies including collisions. Then the GMOs give back the resultant forces to the fluid and the next hydraulic cycle is solved. This interaction between fluid and GMOs is called a "two ways coupling".

The possibility of using periodic boundary conditions reduces the original flume length from 10 meters down to 30 centimetres without any disadvantages. The periodic approach copies all important values from the downstream boundary to the upstream boundary and therefore represents for steady state conditions an infinitely long flume. Due to the structured and orthogonal grid and the use of periodic boundary conditions the computational domain had to be aligned to the horizontal and vertical direction and the gravity vector therefore was split into horizontal and vertical components, depending on the angle of inclination. The original flume width of 30 centimetres were modelled and glued up to 1000 spheres on the numerical flume bottom. The spheres are placed rows shifted in flow direction to model the roughness of a dense packed bed.

The LES approach assumes a highly resolved mesh in order to reproduce over 80% of the kinetic turbulent energy directly and model only the last 20% with a simple Smagorinsky approach.

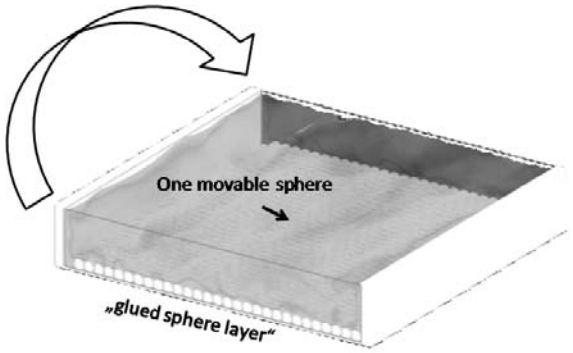

Figure 3: General overview of the numerical model. The periodic boundary condition copies all necessary values from the outlet back to the inlet

Not only the chosen turbulence model requires a very fine mesh but also the geometry of a sphere discretised by a structured grid as used in Flow3D. Figure 4 shows the geometric accuracy depending on the number of mesh cells used for discrete reproduction of the spheres.

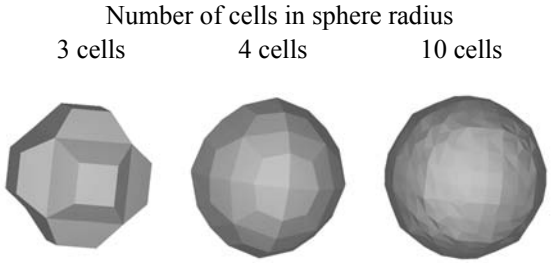

Figure 4: Geometric discretization of an ideal sphere by using the Flow3D FAVOR algorithm to reproduce geometries.

Based on these requirements computations with an equidistant cell resolution of 1x1x1 mm was finally used.

3 SIMULATION OF THE FLOW

LES simulations are quite demanding in CPU time. Therefore the initialization of the computations must be optimized. Therefore the following start up procedure was used for each hydraulic configuration: In a first step the still fluid was set into motion up to steady state conditions using a Reynolds-averaged turbulence model (RANS) (Rodi 1993). Once the steady state was reached the simulation was continued with a LES approach. The change from Reynolds averaging to LES modelling is nicely shown in figure 5. It shows the RANS results for the first 0.5 seconds and later the fluctuations enabled by the LES approach.

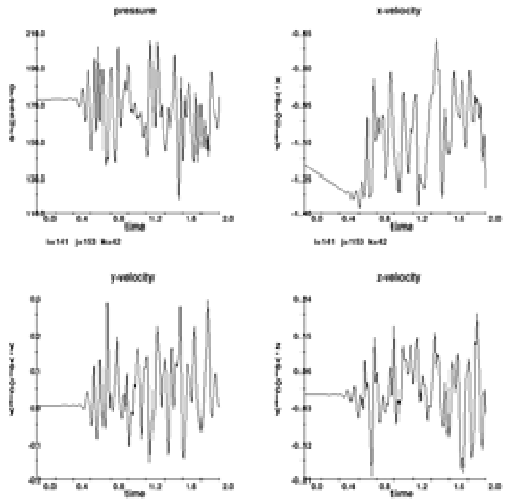

Figure 5: Fluctuations of pressure and velocity components at an exemplary point in the computational domain developing from RANS to LES.

The change in the turbulence modelling is necessary since the RANS averaging does not resolve short-time fluctuations due to turbulence fluctuations. A representative result of flume flow with a RANS approach is illustrated in figure 6. The expected parabolic velocity distribution is absolutely typical for a turbulent flow with RANS over a rough bed.

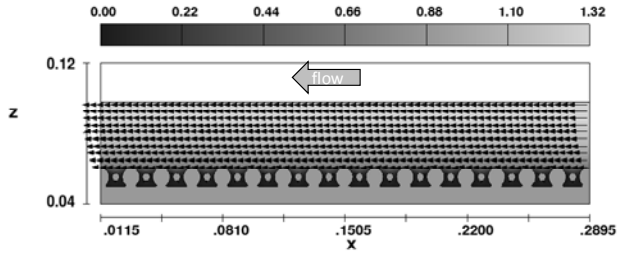

Figure 6: Velocity magnitude (m/s) and vectors of the RANS simulation (pre-run for the LES)

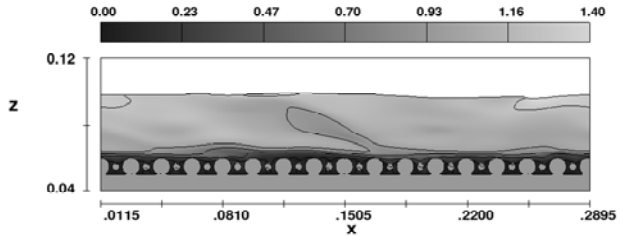

Figure 7: Lateral view of turbulent flow development. Contour shows the velocity magnitude (m/s).

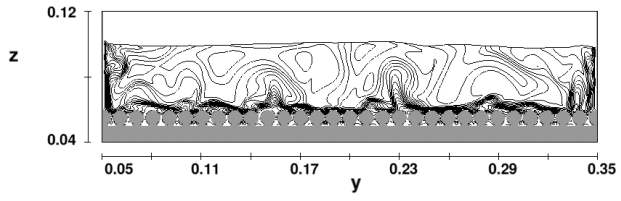

Figure 8: Cross sectional view of velocity contours (isotache) of the LES simulation.

Contrarily, if it is aimed to resolve the fluctuations due to turbulence, as possible with a LES approach, instantaneous flow fields develops as shown in figure 7.

If illustrated in an animation, the observer would realize that the turbulence structures were transported by the flow and therefore point values would vary in time even though the energy in the flow remains constant. Such dynamic variations are the essential key to investigate initialization of bed material as they determine the dynamic loads acting on grains.

To obtain a more detailed understanding of the occurring turbulence structures, figure 9 shows horizontal cuts through the flume. Figure 9a is a cut 0.5 millimetres above the flume bottom. The small circles show the cut planes through the single grains. Figure 9b shows a cut plane near the top of the spheres. Noticeable is the development of differential velocity fields (turbulent structures or "velocity clouds"). Figure 9c shows a cut slightly above the top of the spheres and figure 9d gives a view of the velocity field just below the free surface of the normal flow depth of 4.8 centimetres.

The flow direction in the next figures is from right to left and the contour illustrates the velocity magnitudes in meter per second.

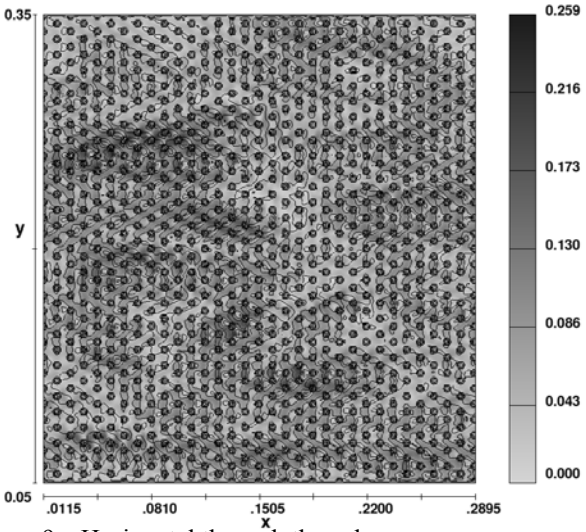

Figure 9a: Horizontal through the spheres

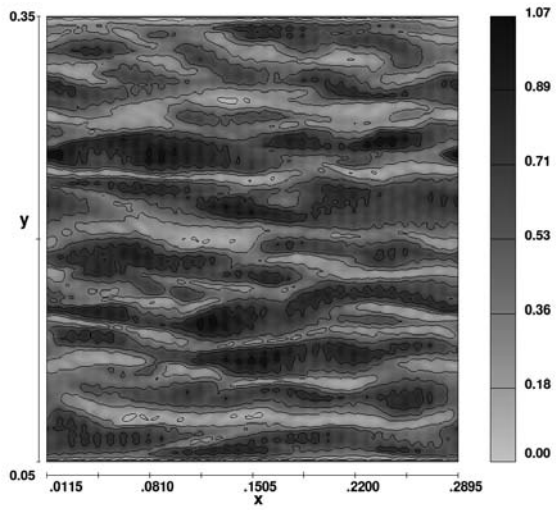

Figure 9b: Horizontal cut, 0.5 mm under top of the spheres

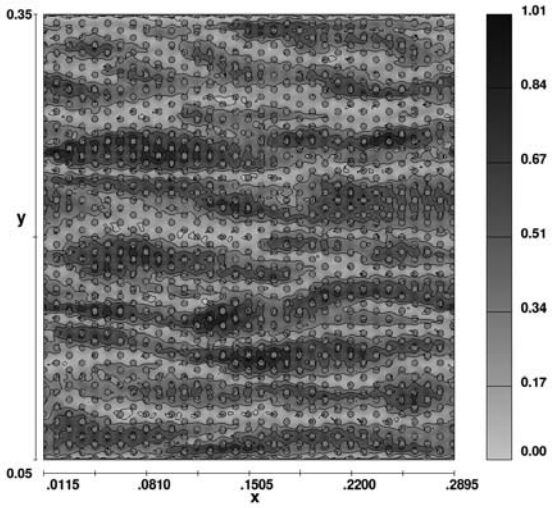

Figure 9c: Horizontal cut, 0.5 mm over top of the spheres

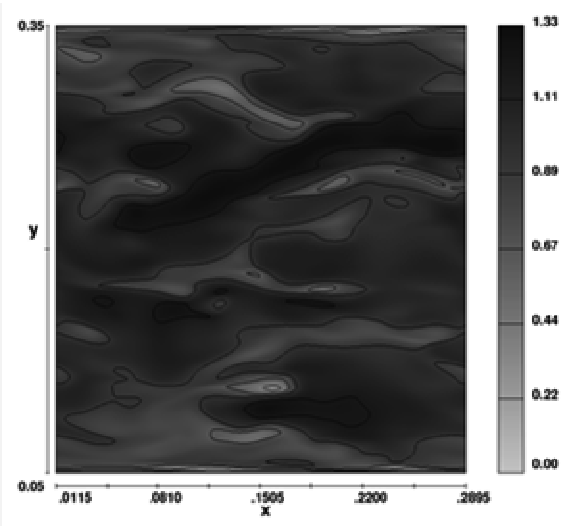

Figure 9d: Horizontal cut close to the free surface

4 INITIAL MOTION OF A SINGLE GRAIN

In the flow field illustrated in figures 9a to 9d, a single movable sphere on a piston were protruded, as experimentally done by Fenton and Abbot (see figure 1). To neglect the vertical momentum, the piston was shifted with a velocity of one millimetre per second only.

Fenton and Abbott performed up to 60 physical tests with differing grain diameters and differing flow conditions. As a start-up, the results of their B1 runs were chosen for the comparison with the numerical results.

The B1 runs represent experiments having a dimensionless Shields number of 0.072, where the Shields number is defined as:

$$\theta_0 = \frac{u_{*0}^2}{g'D} \tag{1}$$

$$g' = g\left(\frac{\rho_s}{\rho - 1}\right) \tag{2}$$

where θ_0 = dimensionless threshold stress, u_x= shear velocity, D = grain diameter, g = gravity acceleration, ρ =density of fluid, ρ_s=density of solid

Fenton and Abbott published for the B1 setup a critical dimensionless exposition of 0.3 The exposition (e) is defined through protrusion divided by diameter.

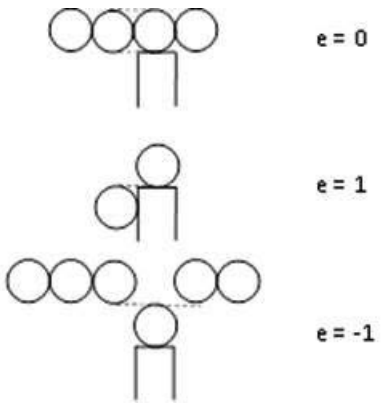

Figure 10: Definition of the exposition

They performed many runs under one setup and published only the minimum value of protrusion, since they wanted to investigate the critical (minimal) shear for initial motion. Similar to Fenton and Abbott a few simulations for identical hydraulic conditions were done. This was achieved by varying only the start point (in time) for motion of the piston using the identical hydraulic simulation. Depending on the choice of the start point the dynamic loading on the single grain is different and load peaks may occur earlier or later (see figure 5). Thus it was chosen to start the piston always one second later than the foregoing run and obtained for each run a different exposition of

the piston and the grain respectively. The following figure shows the results of ten runs of the B1 series.

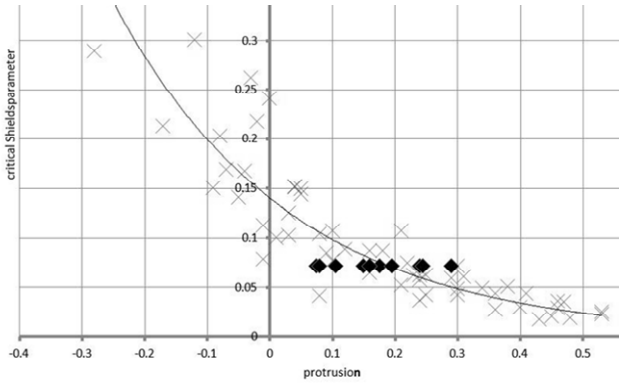

Figure 11: Comparison between the experimental results of Fenton and Abbott and the ten numerical realizations of the B1 setup.

The numerical results fit very nicely with the experiments of Fenton and Abbott. The average of our ten realizations lies perfectly on the trend line of the experiments. Minimum and maximum exposures do also match the experimental results very well meaning that the simulations caught quite nicely the bandwidth of turbulent load fluctuations by the ten realizations even though using always the same LES simulation.

Numerical simulations give the possibility to look in very detail on the physical process of grain lifting. Figure 12 shows a detailed longitudinal cut through the numerical flume where grain and piston are located in the centre of the figure as can be seen from the slight protrusion of the piston.

Figures 12 a) to c) illustrate the detail of initial motion of a single grain for differing times. The range of pressure caption is between 0 and 500 N/m² to give a quantitative indication for the pressure field. (lower pressures are colored black).

Figure 12 clearly shows the lifting effect due to resultant uplift forces. The figures show that the pressure at the top of the grain in figure 12c is negative with a value of -261 N/m². To improve interpretation of the grey scaled images, all negative pressures were colored black. The change of pressure is caused through the turbulent fluctuations of both the velocity and pressure fields. Notable is also the small yet existing velocity field in the pore volume between the spheres. The authors assume that the hydrodynamics of this pore interspace is also very much responsible for initial motion and that the shear model lacks incompleteness. Further analyses will help to gain more insight into these details.

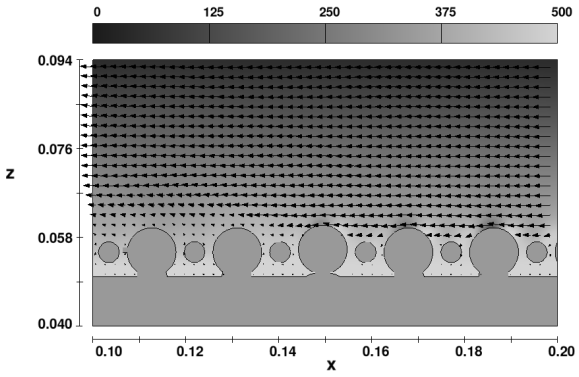

Figure 12 a: lateral view at beginning

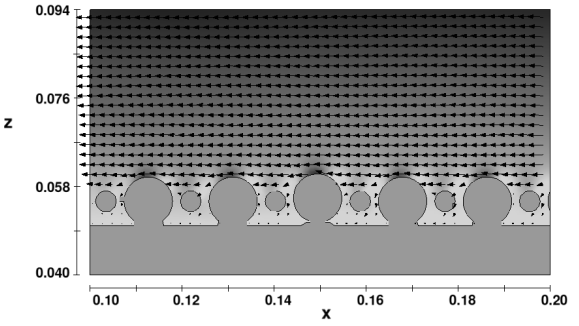

Figure 12 b: lateral view. Dark contours shows hydraulic pressure interaction at spheres

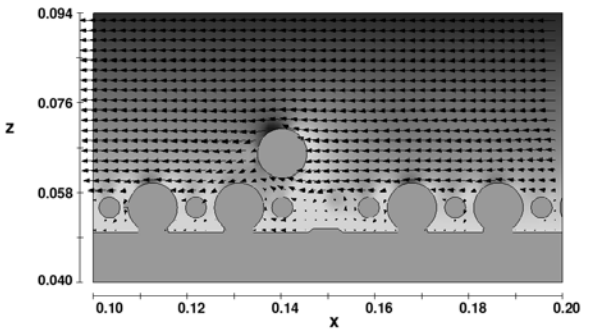

Figure 12 c: lifted sphere

5 RESULTS AND PERSPECTIVE

The initial motion of a grain protruded by a piston into the flow is dependent on various parameters. Time averaged velocities, averaged shear only unsatisfactorily characterize the hydraulic load on a single grain. Besides the geometric parameter of exposure and cross-sectionally averaged flow quantities the range of time-dependent turbulent fluctuations is responsible for initiation of motion of bed load transport.

Therefore the authors believe that the shear force approach traditionally used in bed-load transport is in a physical sense not satisfactory and

suggest reconsidering and thus improving this paradigm.

To predict initial motion, it is important to know, what kind of velocity fields can occur (turbulent energy distribution) and when those "velocity clouds" hit the exposed grains. Such "velocity clouds" of course explain the variation of different exposures for initial motion of grains using identical yet time averaged hydraulic conditions.

Large Eddy Simulations are indispensable to investigate loading forces on single grains. Contrarily to the investigated setup by Fenton and Abbot real bed-load transport is much more complex. Not only one single grain is in motion but many different ones interact with the flow and through collision among themselves. The presented results match very well with the physical results of Fenton and Abbott proofing the suitability to investigate such processes numerically. Nevertheless it will be rather cumbersome and time consuming to proceed and obtain more insight into the physics of sediment motion.

REFERENCES

Braun et al. (2009) "Particle force generation in a turbulent open channel flow" 33th IAHR Congress, Vancouver 2009

Grünzner and Rutschmann (2009) "Initial motion of exposed grains- High resolution LES of Experiments by Fenton and Abbott" 33th IAHR Congress; Vancouver 2009

Fenton and Abbott (1977) "Initial movement of grains on a stream bed: the effect of relative protrusion." Proceeding Royal Society of London A(352): 523-537.

FLOW 3D (2008): FLOW 3D , Flow Science Inc., Santa Fe, USA – online help Version 9.3.1

Rodi, W.(1993). "Turbulence models and their application in hydrauliucs – a state of the art review" IAHR Monograph, 3rd Edition, Balkema, Rotterdam.

Shields, A. (1936). Anwendung der Ähnlichkeitsmechanik und der Turbulenzforschung auf die Geschiebebewegung. Eigenverlag der Preussischen Versuchsanstalt fuer Wasserbau und Schiffbau, Berlin NW 87.